Journal of Fluorescence
https://doi.org/10.1007/s10895-023-03427-5

REVIEW

A 3,5-dinitropyridin-2yl Substituted Flavonol-based Fluorescent Probe for Rapid Detection of H_2S in Water, Foodstuff Samples and Living Cells

Lai-Xin Hong[1] · Rong-Lan Zhang[1] · Jian-She Zhao[1]

Received: 14 August 2023 / Accepted: 1 September 2023

Abstract
A novel flavonol-based fluorescent probe, Fla-DNT, has been synthesized for the rapid and specific detection of H_2S. Fla-DNT exhibits excellent selectivity and anti-interference properties, a short response time (4 min), large Stokes shift (138 nm), and low detection limit (1.357 μM). Upon exposure to H_2S, Fla-DNT displays a remarkable increase in fluorescence intensity at 542 nm. Meanwhile, the recognizing site of H_2S was predicted through Electrostatic potential and ADCH charges calculations, while the sensing mechanism of H_2S was determined via HRMS analysis and DFT calculation. More importantly, the probe owes multiple applications, such as a recovery rate ranging from 92.00 to 102.10% for detecting H_2S in water samples, and it can be fabricated into fluorescent strips to track H_2S production during food spoilage by tracking color changes, thereby enabling real-time monitoring of food freshness. The bioimaging experiments demonstrate the capability of Fla-DNT to detect both endogenous and exogenous H_2S in living cells. These results provide a reliable method and idea for H_2S detection in complex environments.

Keywords Hydrogen sulfide · Ultrasensitive · Water samples · Foodstuff · Bioimaging

Introduction

Hydrogen sulfide (H_2S), a toxic gas, possesses an odor that is reminiscent of rotten eggs [1–3]. Significant quantities of H_2S can be generated during food spoilage, which is produced through the decomposition of sulfur-containing substances by bacteria such as Shewanella putrefaciens, Pseudomonas mephitica, and Citrobacter freundii [4, 5]. Therefore, the release level of H_2S serves as a crucial indicator for monitoring the freshness and quality of food products. There is compelling evidence indicating that the excessive production of H_2S in raw meat has a detrimental impact on both food quality and human health [6, 7]. Additionally, discharging industrial wastewater containing excessive amounts of H_2S can pose potential risks to both aquatic life and human health [8, 9]. Although H_2S is commonly considered a toxic gas molecule, it has been identified as the third gas signaling molecule following nitric oxide (NO) and carbon monoxide (CO) [10]. In mammals, endogenous H_2S plays crucial biological roles in terms of its anti-inflammatory properties, regulation of the immune system, and modulation of cardiovascular function. However, dysregulated levels of H_2S have been associated with various pathological diseases, such as diabetes, cirrhosis, Alzheimer's disease and even cancer [11–14]. Therefore, it is imperative to develop a highly sensitive and selectively reliable technique for the assessment of H_2S levels in food and biological samples.

Recently, responsive fluorescent probes have emerged as an ideal approach for in situ and in vivo measurement of H_2S due to their inherent advantages of convenient operation, non-destructive analysis, high sensitivity and selectivity [15–22]. These probes capture H_2S through various special reaction mechanisms such as nucleophilic attack [23], copper sulfide precipitation [1], and azide reduction [24]. The fluorescence technique has been widely utilized in diverse fields, encompassing environmental water sample monitoring, food inspection, and biological imaging. For instance, Diao et al. [25] developed a ratiometric fluorescent probe that enables the detection of both endogenous and

✉ Rong-Lan Zhang
zhangrl@nwu.edu.cn

[1] Key Laboratory of Synthetic and Natural Functional Molecule of the Ministry of Education, Xi'an Key Laboratory of Functional Supramolecular Structure and Materials, College of Chemistry and Materials Science, Northwest University, Xi'an 710069, Shaanxi, PR China

Published online: 06 September 2023

exogenous H_2S in living cells. Zhu et al. [26] constructed a fluorescent probe based on Rhodamine B and fluorescein for the detection of H_2S, which was successfully applied to visualize H_2S in MCF-7 cells and Caenorhabditis elegans. Zhou et al. [27] designed a water-soluble fluorescent probe that not only enables bioimaging of H_2S in Hela cells but also can sense H_2S gas generated from food spoilage by incorporating fluorescent test strips loaded with probes for monitoring food freshness. Despite the development of various fluorescent probes for H_2S detection, most of them still suffer from limitations such as severe self-absorption, prolonged response time, and inability to detect gaseous H_2S. In view of these constraints, we designed a fluorescent probe with excellent spectral properties and practical application value that can be effectively employed for the detection of H_2S gases in complex environments.

Herein, an H_2S-specific probe (Fla-DNT) was designed based on the thiolysis reaction as the design strategy. The fluorophore 4-dimethylaminoflavonol (Fla), which possesses excellent optical stability and a large fluorescence quantum yield, was incorporated with a specific H_2S-reactive group, 3,5-Dinitropyridine-2-yl (DNT), for sensitive and selective detection of H_2S. The DNT group was introduced to Fla as an electron acceptor, inducing fluorescence quenching of the probe through the photoinduced electron transfer (PET) effect. Upon treatment with H_2S, nucleophilic substitution reaction of Fla-DNT occurred and the free fluorophore was released, resulting in enhanced fluorescence due to the inhibition of the PET process. Subsequently, a comprehensive evaluation of the spectral properties and H_2S responsiveness of Fla-DNT was conducted. Biological experiments demonstrate that Fla-DNT exhibits excellent biocompatibility and can image both endogenous and exogenous H_2S in living cells. More importantly, Fla-DNT successfully detected the H_2S in environmental water samples and food spoilage, indicating the potential application of this probe in several fields.

Result and Discussion

Fla-DNT Synthesis and Characterization

The H_2S fluorescent probe Fla-DNT was designed initially here. 4-dimethylaminoflavonol (Fla) and 3,5-Dinitropyridine-2-yl (DNT) underwent the etherification reaction to synthesize Fla-DNT (**Scheme S1**), which is a common nucleophilic substitution reaction. The protection–deprotection of functional groups often leads to changes in electronic properties. Due to the strong quenching effect of the DNT moiety, it was anticipated that Fla-DNT would exhibit negligible fluorescence and large Stokes shift (Fig. S1). The structure characterizations of Fla-DNT are presented in Fig. S2-S4.

Optical Properties

The responsiveness of Fla-DNT towards H_2S was evaluated in PBS buffer solution (pH 7.4, 10 mM, 10% DMSO). As depicted in Fig. 1, it is evident that Fla-DNT displays a maximum absorption band at approximately 397 nm and possesses inherently non-fluorescent properties. Upon the addition of H_2S, the maximum absorption band gradually shifts to 7 nm with strong fluorescence emission at 542 nm. This redshift can be attributed to the presence of non-bonding electrons in the hydroxyl group, and the conjugation effect of p-π with the carbon-carbon double bond leads to the reduced energy of the π→π* transition. Simultaneously, the solution undergoes a color change from off-white to yellow upon exposure to sunlight, accompanied by intense green fluorescence under 356 nm excitation that is discernible with the naked eye. These results collectively demonstrate the potential of Fla-DNT as a fluorescent "turn-on" probe for detecting H_2S. When 10 equiv H_2S was added, the kinetic analysis (Fig. 2) revealed that the fluorescence intensity was gradually enhanced with an increased reaction time. The fluorescence intensity reaches saturation and stability within 4 min but exhibits 30-fold enhancement. Analysis of fluorescence data demonstrates a good linear

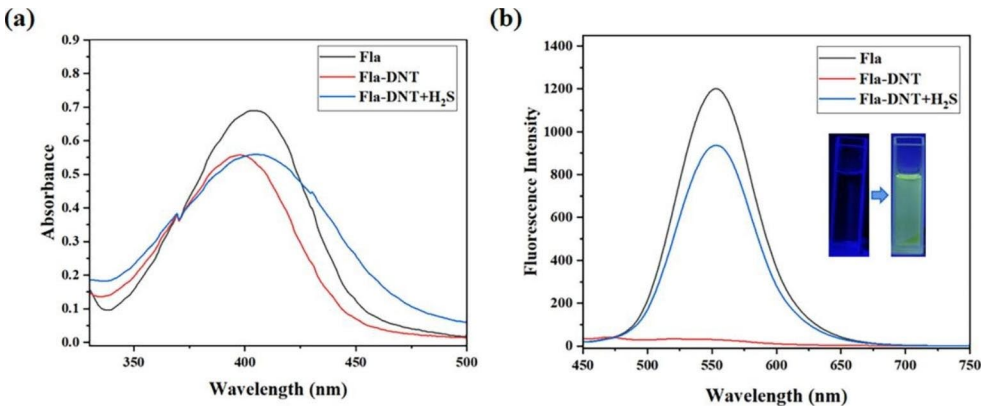

Fig. 1 (**a**) Comparison of absorbance for 20 μM Fla-DNT in the presence and absence of 200 μM H_2S. (**b**) Fluorescence spectral changes of probe Fla-DNT (20 μM) upon addition of H_2S (200 μM)

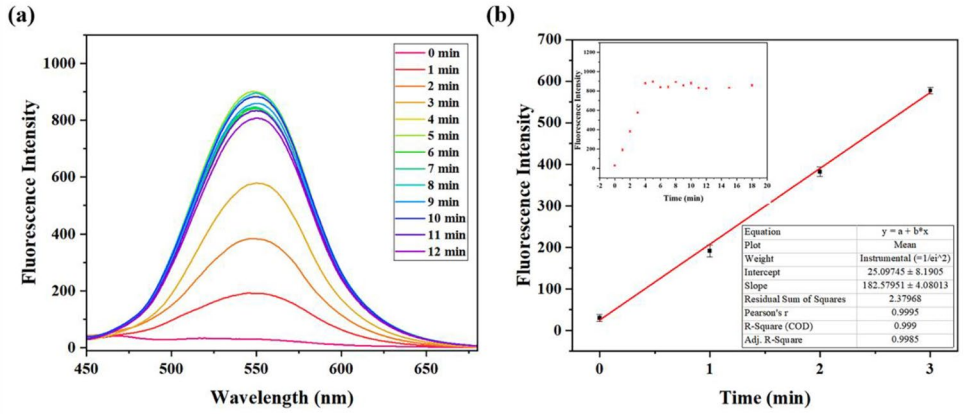

Fig. 2 (**a**) The fluorescence intensity changes with time for 20 µM Fla-DNT in the presence of 200 µM H_2S. (**b**) Linearly increased fluorescent intensity at 542 nm from 0 to 3 min. A fluorescence saturation curve at 542 nm is shown in the inset

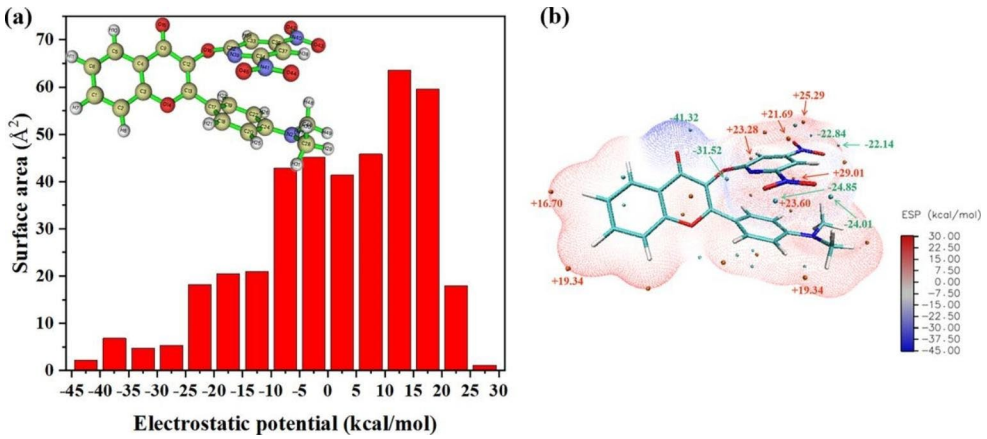

Fig. 3 (**a**) Surface area in each ESP ranges on the vdW surface of Fla-DNT. Insert: structure and atomic number of the Fla-DNT molecule. (**b**) ESP-mapped molecular vdW surface of Fla-DNT with surface local minima and maxima of ESP are represented as green and orange spheres, respectively. Partial surface local minima and maxima of ESP are marked in the figure, where the maximum and minimum values are highlighted in italics

correlation between fluorescence intensity and time within the range of 0–3 min (Fl = 182.58t + 25.08, $R^2 = 0.9985$), indicating that Fla-DNT possesses rapid detection capability for H_2S.

Proposed Mechanism

Interestingly, the absorption and emission spectra of Fla-DNT solution added H_2S were found to be similar to those of Fla. Therefore, we speculate that Fla is generated in this process. Initially, Gaussian 16 software was utilized to optimize the molecular structure based on the quantum chemistry Density Functional Theory (DFT) at the B3LYP/6-31G(d) level, resulting in obtaining stable structure and wave function files. Multiwfn 3.7 was employed to calculate the Electrostatic potential (ESP) on the molecular vdW surface and atomic dipole corrected Hirshfeld atomic charge (ADCH) of Fla-DNT to determine which carbon is most likely to serve as the reaction site [28–30]. The majority of ESP analyses are performed on the molecular vdW surface, and atoms located near the maximum point of ESP on this surface are more susceptible to attack by nucleophiles. As illustrated in Fig. 3a, among all the extreme points (including 17 maxima and 15 minimum), C32 exhibits the largest ESP value and is theoretically considered as the most reactive. The distribution surface area map of ESP values on vdW surface indicates that they are mainly distributed between −40 to +25 kcal/mol. However, the distribution area (greater than 25 kcal/mol) determining the nucleophilic reaction sites is relatively concentrated, indicating that the reaction site is also more concentrated. The ADCH charges were further computed to investigate the charge distribution of each atom in Fla-DNT (Table S1). The sites of nucleophilic and electrophilic reactions are often determined by the electrical properties and quantities carried by the atoms, with negatively charged nucleophiles preferring to attack atoms with higher positive charges [31]. Figure 3b indicates that the ADCH charge value of the C32 atom is the largest of all atoms except the N40 and N41 (due to the stability of the nitro structure conjugated with benzene ring), implying its high susceptibility towards nucleophiles. The aforementioned computational results strongly suggest that C32 serves as the most reactive site for HS^- nucleophilic attack.

Theoretical Calculation

To better explain the fluorescence "turn on" and "turn off" during H_2S tracking, DFT calculations of Fla, DNT,

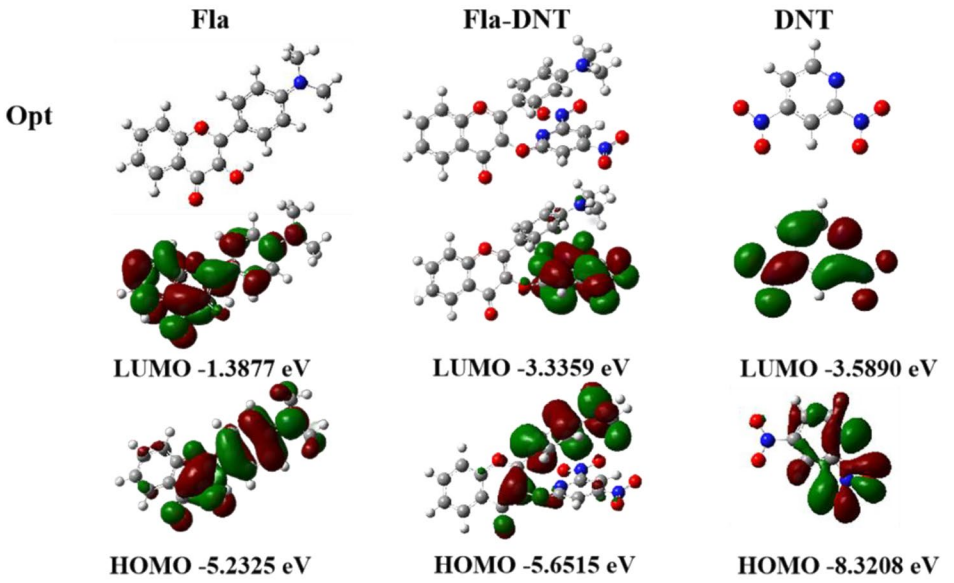

Fig. 4 The optimized structures of Fla, Fla-DNT and DNT in the first row. The frontier molecular orbitals (MOs) of Fla, Fla-DNP and DNP based on density functional theory (DFT) calculations in the remaining rows. The the ball-and-stick model depicts carbon, hydrogen, oxygen and nitrogen atoms as gray, write, red and blue spheres, respectively

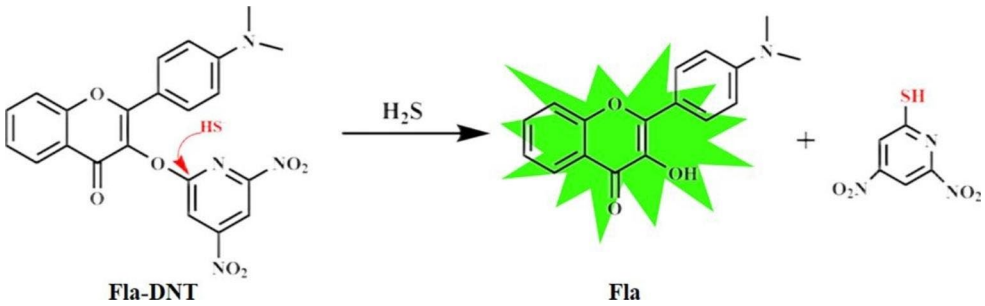

Fig. 5 The proposed reaction mechanism of Fla-DNT towards H_2S.

and Fla-DNT were carried out using Gaussian 16 using B3LYP/6-31G(d) basis set. As shown in Fig. 4, the HOMO of the Fla-DNT molecule is predominantly situated in the 3-hydroxyflavonoid moiety, while the LUMO is primarily located in the 3,5-dinitropyridin-2-yl moiety. The computational results reveal that the LUMO energy level (-3.5890 eV) of the DNT group is positioned between the HOMO (-5.6515 eV) and LUMO (-3.3359 eV) orbital of Fla-DNT. Therefore, when Fla-DNT is excited, electrons can be transferred from the 3-hydroxyflavonoid moiety (PET donor) to the 3,5-dinitropyridin-2-yl moiety (PET acceptor), thereby initiating the remarkable PET process resulting in fluorescence quenching. However, in the presence of H_2S, Fla-DNT is nucleophilic attacked by HS^- and is converted to Fla. Both HOMO and LUMO are mainly localized on the fluorescent backbone, thereby preventing electron transfer processes. Consequently, the fluorescence remains in the "turn-on" state. The aforementioned above data illustrates the proposed fluorescence spectral response mechanism depicted in Fig. 5.

The reactive site and sensing mechanism were determined by HRMS. Mass spectrometry characterization (Fig. S5) revealed a prominent peak at m/z: 281.1120 [M + H] corresponding to Fla. Based on the above information, the process of H_2S sensing by the Fla-DNT is illustrated in Fig. 5. During the recognition, the carbon atom linked to oxygen in the recognition group was specifically nucleophilic attacked by HS^-, leading to thiolysis and release of fluorophore Fla. Simultaneously inhibiting the PET process results in fluorescence activation, thereby realizing a change in fluorescence signal.

Selective and Anti-interference Ability

The selectivity of Fla-DNT towards H_2S was investigated using fluorescence spectroscopy. We assessed the reactivity of Fla-DNT towards various potential interfering agents, including H_2S, common cations (Na^+, Ni^{2+}, Al^{3+}, Ca^{2+}, NH_4^+, Fe^{3+}, Zn^{2+}, K^+, Co^{2+} and Mn^{2+}), anions (SO_3^{2-}, NO_3^-, SO_4^{2-}, Cl^-, Br^-, HCO_3^-, NO_2^-, CO_3^{2-}, SCN^-, F^- and I^-), amino acids (Trp, Leu, Try, Gly, Phe, Lys, Arg, Val, Pro, Cys, Hcy and GSH) and reactive oxygen species (ROS). As expected, Fla-DNT exhibits obvious fluorescence enhancement at 542 nm only when incubated with H_2S, while other substances fail to induce any noticeable changes (Fig. S6). It is noteworthy that the fluorescence changes caused by

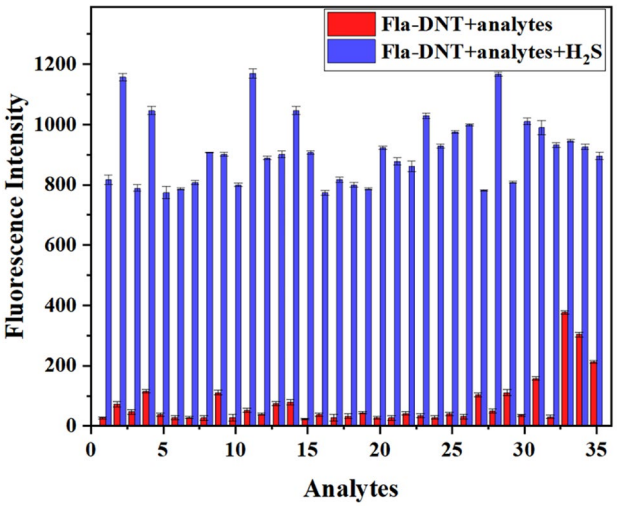

Fig. 6 Fluorescence responses of Fla-DNP (20 μM) at 542 nm toward various analytes. Red bars indicate single analyte additions, which are (1) Na^+, (2) Ni^{2+}, (3) Al^{3+}, (4) Ca^{2+}, (5) NH_4^+, (6) Fe^{3+}, (7) Zn^{2+}, (8) K^+, (9) Co^{2+},(10) Mn^{2+}, (11) SO_3^{2-}, (12) NO_3^-, (13) SO_4^{2-}, (14) Cl^-, (15) Br^-, (16) HCO_3^-, (17) NO_2^-, (18) CO_3^{2-}, (19) SCN^-, (20) F^-, (21) I^-, (22) Trp, (23) Leu, (24) Try, (25) Gly, (26) Phe, (27) Lys, (28) Arg, (29) Val, (30) Pro, (31) ROS, (32) blank, (33) Cys, (34) Hcy, (35) GSH. Green bars indicate the subsequent addition of H_2S (200 μm) to the mixture

biothiols are negligible compared to those induced by H_2S. These findings indicate that Fla-DNT is an excellent selective probe for detecting H_2S.

Anti-interference ability is a crucial parameter for assessing the performance of fluorescent probes. Therefore, the competition assay was conducted by adding H_2S to solutions containing Fla-DNT and other analytes to further validate the selectivity of Fla-DNT for H_2S. The competitive experiments (Fig. 6) demonstrate that the presence of interfering analytes has no impact on the identification of H_2S by Fla-DNT, as evidenced by nearly identical fluorescence-enhancing signals. It is apparent that Fla-DNT holds promise for detecting H_2S in complex conditions.

pH and Sensitivity

As pH is also an important reaction process factor, the impact of pH was examined in the presence or absence of H_2S over the range of pH 2.0 to 9.0 (Fig. S7). The fluorescence intensity of Fla-DNT remained stable within the range of pH 2.0 ~ 7.0 and slightly increased from 8.0 to 9.0, which may be attributed to nucleophilic attack by OH^- on the strong electron-withdrawing group DNT. After the addition of 10 equiv. H_2S, a significant increase in fluorescence was observed at 542 nm within the pH range of 5.0 to 7.0, which stabilized beyond pH 8.0. The above results demonstrate that Fla-DNT is capable of detecting H_2S over a wide pH and has the potential for practical application in monitoring physiological levels of H_2S.

The sensitivity of Fla-DNT to H_2S was further investigated through fluorescence titration experiments, wherein varying concentrations of H_2S (0-400 μM) were utilized to react with Fla-DNT (20 μM) at room temperature. As shown in Fig. 7, a progressive increase in fluorescence intensity at 542 nm is observed when the H_2S concentration ranges from 0 to 20 μM. A linear relationship is observed between fluorescence intensity and H_2S concentrations, with the equation of $Fl = 44.4[H_2S] + 31.5$, indicating excellent correlation. It demonstrates that Fla-DNT possesses both qualitative and quantitative sensing capabilities for H_2S. However, recognition of H_2S by Fla-DNT reaches saturation at concentrations exceeding 60 μM, and the fluorescence intensity remains almost unchanged. Based on the equation of 3σ/k, Fla-DNT exhibits an impressively low detection limit (LOD) of 1.357 μM for H_2S, which indicates that Fla-DNT can be applied to detect H_2S with high sensitivity.

Environmental Water Sample Application

In order to validate the practical applicability of Fla-DNT in the environment, the fluorescence emission spectra were obtained from various water samples (Xi'an moat water,

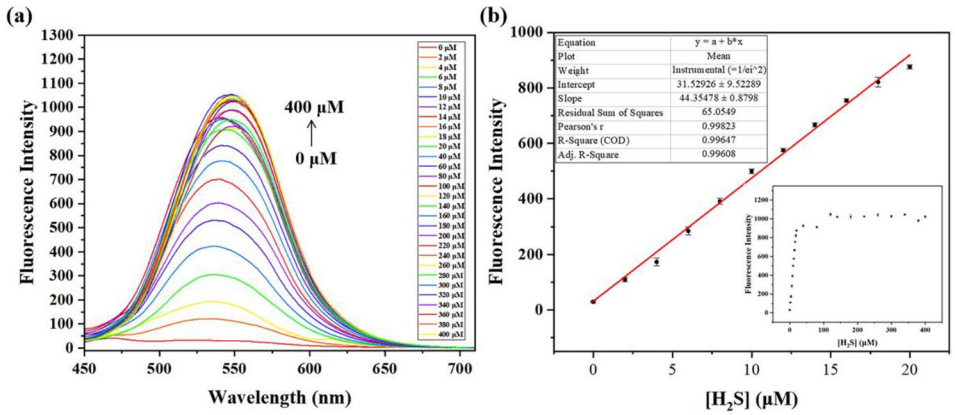

Fig. 7 (**a**) Fluorescent spectral changes of Fla-DNP (20 μM) upon addition of different concentrations of H_2S (0-400 μM). (**b**) Linearly increased fluorescent intensity at 542 nm from 0 to 16 μM. Insert: a fluorescence saturation curve at 542 nm

tap water and deionized water) using the standard addition method. Specifically, Fla-DNT (20 μM) was added separately to the mixed solution containing different concentrations of Na_2S. The results demonstrate a strong linear relationship between the fluorescence intensity and the concentration of Na_2S within the range of 0–20 μM in Fig. S8. The recoveries of Fla-DNT in three water samples were determined to closely match the actual addition concentration of Na_2S, with a recovery rate ranging from 92.00 to 102.10% (Table 1). These monitoring results illustrate that Fla-DNT can analyze H_2S in real water samples with high accuracy.

Test Strips Experiments

The obvious fluorescence response of Fla-DNT to H_2S in solution has motivated us to explore its potential applications. As a result, a fluorescent test strip loaded with Fla-DNT was designed for the real-time monitoring of both gaseous and aqueous H_2S. The dried fluorescence test strips were immersed in different concentrations of Na_2S solution (0 μM, 4 μM, 40 μM, 400 μM) for 1 min. Subsequently, the color variation was observed under the 365 nm lamp. It is evident that the green fluorescence of the test strips increased in a dose-dependent manner with H_2S concentration. Even at 0.1 eq. Na_2S, the fluorescence change is observable to the naked eye (Fig. S9a). Shockingly, the test strips were capable of detecting H_2S gas (produced from Na_2S and HCl) within a short period, with the green fluorescence of test strips exposed to high concentrations of H_2S being more pronounced (Fig. S9b). It is evident that the Fla-DNT-based strip represents a portable and visually discernible tool.

Table 1 Analytical results of Fla-DNT in real water samples

Samples	Na_2S spiked (μM)	Na_2S recovered (μM)	recovery (%)
Tap water	0	Not detected	——
	4	3.69 ± 0.06	92.25%
	8	7.85 ± 0.12	98.13%
	12	11.90 ± 0.09	99.17%
	16	16.04 ± 0.04	100.25%
	20	20.15 ± 0.07	102.10%
River water	0	Not detected	——
	4	3.68 ± 0.04	92.00%
	8	7.80 ± 0.09	97.50%
	12	11.89 ± 0.21	99.08%
	16	16.03 ± 0.04	100.19%
	20	20.18 ± 0.16	100.90%
Deionized water	0	Not detected	——
	4	3.72 ± 0.04	93.00%
	8	7.79 ± 0.01	97.38%
	12	11.88 ± 0.07	99.00%
	16	16.07 ± 0.09	100.44%
	20	20.14 ± 0.22	100.70%

Analysis in Food Samples

The outstanding performance of fluorescent test strips loaded with Fla-DNT has inspired us to develop its practical application for the detection of H_2S generation during food spoilage. As the release level of H_2S is regarded as an indicator of the quality of raw meat [32], monitoring changes in fluorescence signals on test strips can enable real-time assessment of food freshness. As depicted in Fig. 8, when the food samples were stored at 40 °C, the green fluorescence exhibited a progressive enhancement over time on the strips, indicating that spoilage had occurred and the food was unsuitable for consumption. In the control group (Fig. S10), storing the food samples at 4 °C for 48 h resulted in only a slight change in fluorescence intensity on the test strips, suggesting that low temperature can mitigate the rate of deterioration in raw meat to some extent. The above experiments reveal the probes prepared into test strips have practical application value in tracking the H_2S produced during food spoilage.

Cytotoxicity and Bioimaging

Encouraged by the excellent sensing properties of Fla-DNT towards H_2S, the investigation was further conducted to explore its feasibility as a probe for imaging H_2S in living cells. The cell viability of 4T1 cells treated with different concentrations of Fla-DNT (0, 10, 20, 30, 40, 50 μM) for 24 h was assessed using MTT assay. As depicted in Fig. S11, the results demonstrate that even at a concentration of 50 μM, the cell viability remained above 90%, indicating the excellent biocompatibility and low toxicity of the probe.

Subsequently, cell imaging experiments of Fla-DNT monitoring H_2S were performed (Fig. 9). Compared with the control group, a weak fluorescence signal was detected after 30 min of co-incubation of cells with Fla-DNT (30 μM), and the process of fluorescence turning-on was realized. Moreover, when cells are treated with Fla-DNT followed by continued incubation with exogenous H_2S (5 μM and 20 μM) for 1 h, significant fluorescence enhancement with the increase of Na_2S concentration can be observed inside the cells. The results of cell imaging experiments demonstrate that Fla-DNT not only exhibits excellent cell membrane permeability but also possesses the capability to detect endogenous and exogenous hydrogen sulfide in living cells. These findings suggest that Fla-DNP represents a highly effective tool for monitoring and imaging H_2S.

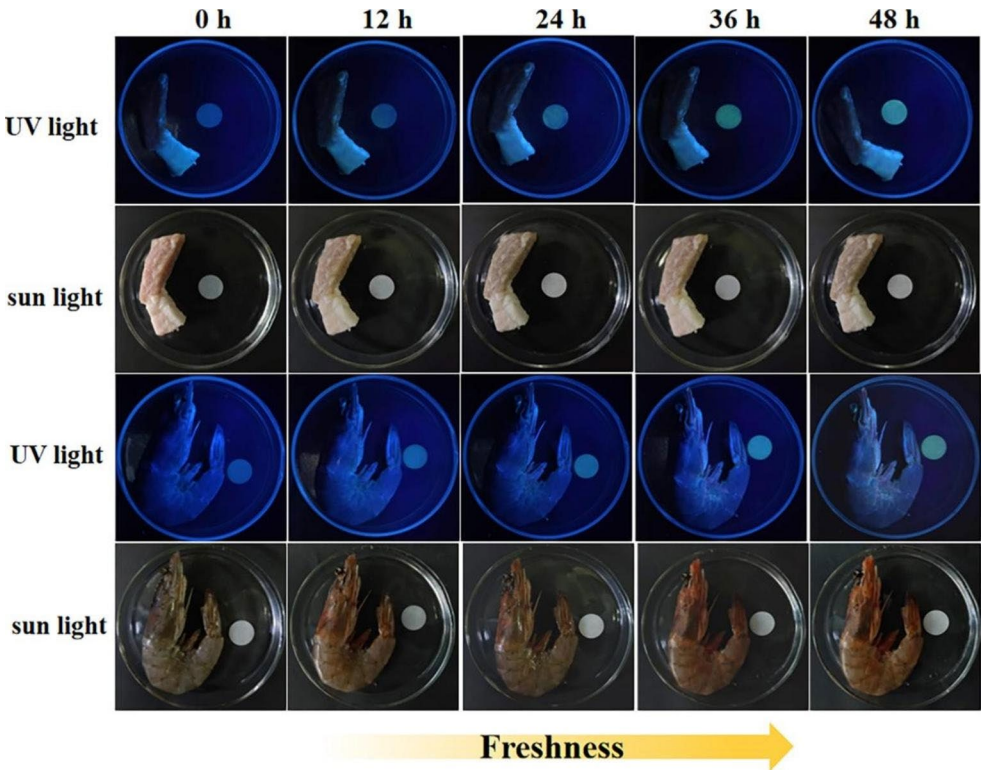

Fig. 8 Test strips of the Fla-DNT for detecting of H_2S generated during a) pork, b)shrimp spoilage at 40 ºC

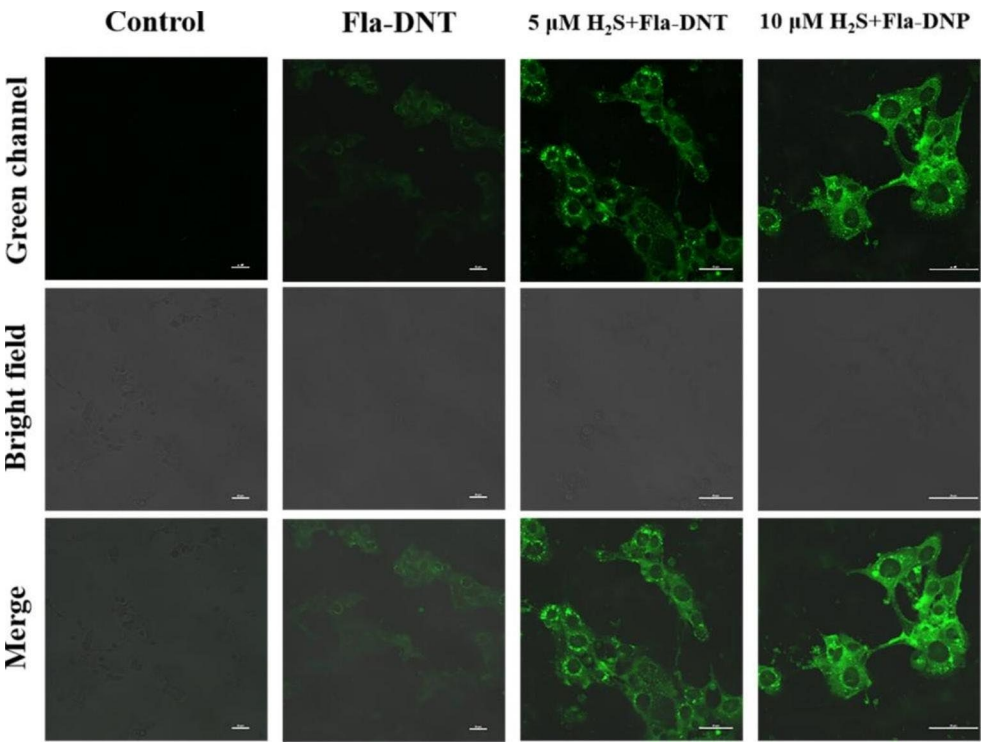

Fig. 9 Confocal imaging of H_2S in 4T1 cells with probe Fla-DNT. (a) cell blank, (b) 4T1 cells only were treated with probe Fla-DNT (30 μM) for 30 min, 4T1 cells were incubated with probe Fla-DNT (30 μM) for 30 min and then treated with (c) 5 μM and (d) 20 μM Na_2S for 1 h (λex = 488 nm, green channel: λem = 500–550 nm, scale bar: 50 μm)

Conclusion

In summary, we have successfully synthesized a fluorescent probe for H_2S detection based on 3,5-dinitropyridin-2yl substituted flavonol. After treatment with H_2S, the DNT group of the probe undergoes nucleophilic attack by HS^-, leading to release the fluorophore Fla and accompanied by strong green fluorescence emission signal. Notably, Fla-DNT exhibits a satisfactory response rate (4 min) and detection limit (1.357 μM), while effectively detecting gaseous H_2S. More importantly, the probe has demonstrated its wide practical value and promising prospects by successfully detecting H_2S in water, foodstuff samples, and living cells.

Experimental Section

Materials and Apparatus

Materials and apparatus were described in Supporting Information.

Synthesis of Fla-DNP

Anhydrous K_2CO_3 (69.1 mg, 0.5 mmol) was introduced into the DMF (5 mL) solution containing Fla (100 mg, 0.355 mmol) at room temperature and stirred for 30 min, followed by the addition of 2-Chloro-3,5-dinitropyridine (72.2 mg, 0.355 mmol). The mixture was stirred continuously for 3.5 h until sufficient reaction had occurred before being poured into an ice-water mixture to precipitate solid substances which were then filtered and further purified by column chromatography. TLC analysis on a silica plate was performed. TLC (silica plate): Rf 0.56 (Petroleum ether-ethyl acetate 5: 1, v/v); Yield: 78%. ^{1}HNMR (400 MHz, Chloroform-d) δ 9.20, 9.07, 8.18 (d, J = 7.9 Hz), 8.11–7.98 (m), 7.72 (d, J = 7.3 Hz), 7.62 (d, J = 8.4 Hz), 7.43, 6.75 (dd, J = 9.1, 3.6 Hz), 3.06. HRMS (ESI-TOF) Calcd for Fla-DNT $[M+H]^+$:449.1091, found: 449.1071.

Preparation of Solutions

The stock solution of Fla-DNT (400 μM) was prepared in DMSO, while the cations (Na^+, Ni^{2+}, Al^{3+}, Ca^{2+}, NH_4^+, Fe^{3+}, Zn^{2+}, K^+, Co^{2+} and Mn^{2+}), anions (S^{2-}, SO_3^{2-}, NO_3^-, SO_4^{2-}, Cl^-, Br^-, HCO_3^-, NO_2^-, CO_3^{2-}, SCN^-, F^- and I^-) and amino acids (Trp, Leu, Try, Gly, Phe, Lys, Arg, Val, Pro, Cys, Hcy and GSH) stock solutions (1 mM each) were prepared in distilled water.

Spectroscopic Measurements

All absorption and emission spectra were collected in PBS buffer solution containing 10% DMSO at pH 7.4 and room temperature. Unless otherwise stated, the concentration of Fla-DNT was 20 μM and the time was recorded at 5 min after adding analytes. The fluorescence spectra were excited at 400 nm (slit widths: 5 nm/10 nm).

Real Water Samples Assay

The Xi'an moat water, tap water and deionized water samples were collected for the recovery test. The impurities in the water samples were eliminated using a 0.22 μm microfiltration membrane. Prior to adding different concentrations of Na_2S (0, 4.0, 8.0, 12.0, 16.0, 20.0 μM), the pH of each sample was adjusted to 7.4 with PBS buffer solution.

Preparation of Test Strips

The filter paper was cut into circular test strips, which were then immersed in DMSO solution of Fla-DNT (40 μM) and dried to remove the solvent. The resulting strips were subjected to sensing experiments using different concentrations of Na_2S solution and H_2S vapor.

Testing of Raw Meat Samples

Food samples (pork and shrimp) were procured from the supermarket, washed with distilled water and cut into uniform pieces. The meat samples and Fla-DNT-containing test strips were enclosed in sealed Petri dishes. Fluorescence images were collected under sunlight and at 365 nm UV light at different times (0 h, 12 h, 24 h, 36 h, 48 h). Control experiments were conducted by monitoring the fluorescence signal changes in a refrigerated environment maintained at 4 °C.

Cytotoxicity

The 4T1 cells were cultured in culture medium supplemented with 10% fetal bovine serum (FBS) and incubated at 37°C in a 5% CO_2 atmosphere. To determine the cytotoxicity of Fla-DNT, MTT assays were performed. Specifically, the 4T1 cells were seeded into 96-well plates (10,000/well) and allowed to adhere for 24 h. Subsequently, the cells were treated with a series of concentrations of Fla-DNT (0, 10, 20, 30, 40, 50 μM) for another 24 h. After removing the sample solution and washing the cells thoroughly, a 20.0 μL MTT dye solution (5.0 mg/mL) was added to the cells and incubated for 4 h. Subsequently, 100 μL DMSO was

injected to fully dissolve the formazan crystals, and the optical density was obtained using a microplate reader.

Living Cells Imaging

Four groups of 4T1 cells were cultured in confocal dishes to a density of 1000/cm^2. The control group remained untreated, while the other three groups were incubated with Fla-DNT (20 μM) for 30 min at 37 ℃. In two of these groups, Na_2S was introduced at different concentrations (5 and 20 μM) after adding Fla-DNT respectively, and the cells continued to incubate for 60 min. Finally, the four groups were washed three times with PBS buffer to discard the culture medium before fluorescence images were captured with a confocal microscope.

Supplementary Information The online version contains supplementary material available at https://doi.org/10.1007/s10895-023-03427-5.

Author Contributions All authors contributed to the study conception and design. Material preparation, data collection and analysis were performed by Laixin Hong. The first draft of the manuscript was written by Laixin Hong and all authors commented on previous versions of the manuscript. All authors read and approved the final manuscript.

Funding The authors is grateful for the financial support from the Key Research and Development Project of Shaanxi Province (No. 2022GY-375) and Open Fund Project of Xi'an Key Laboratory of Functional Supramolecular Structure and Materials (No. CFZKFKT23006) for the financial support of this work, and the authors thank Prof. Bingbing Suo (Institute of Modern Physics, Northwest University) for supplying the Gaussion 16 simulation package.

Data Availability The data generated and analyzed will be made available upon reasonable request from the corresponding authors.

Declarations

Competing interests The authors declare no competing interests.

Ethics approval and consent to participate The study was performed in strict accordance with the guidelines of the Animal Ethical and Welfare Committee of Northwest University.

References

1. Li L, Rose P, Moore P (2011) Hydrogen sulfide and cell signaling. Annu Rev Pharmacol 51:169–187
2. Wang R (2002) Two's company, three's a crowd: can H_2S be the third endogenous gaseous transmitter? Faseb J 16:1792–1798
3. Li L, Moore P (2008) Putative biological roles of hydrogen sulfide in health and disease: a breath of not so fresh air? Trends Pharmacol Sci 29:84–90
4. Koskela J, Sarfraz J, Ihalainen P, Määttänen A, Pulkkinen P, Tenhu H, Nieminen T, Kilpelä A, Peltonen J (2015) Monitoring the quality of raw poultry by detecting hydrogen sulfide with printed sensors. Sens Actuators B Chem 218:89–96
5. Yang X, Lu X, Wang J, ,Wang J, Zhang Z, Du X, Zhang J, Wang J (2022) Near-Infrared fluorescent probe with a large Stokes Shift for detection of Hydrogen Sulfide in Food Spoilage, living cells, and zebrafish. J Agric Food Chem 70:3047–3055
6. Muthusamy S, Rajalakshmi K, Zhu D, Zhao L, Wang S, Zhu W (2020) A novel lysosome targeted fluorophore for H_2S sensing: enhancing the quantitative detection with successive reaction sites. Sens Actuators B Chem 320:128433–128440
7. Xiao P, Liu J, Wang Z, Tao F, Yang L, Yuan G, Sun W, Zhang X (2021) A color turnon fluorescent probe for real-time detection of hydrogen sulfide and identification of food spoilage. Chem Commun 57:5012–5015
8. Wing S, Wolf S (2000) Intensive livestock operations, health, and quality of life among eastern North Carolina residents. Environ Health Persp 108:233–238
9. Muthusamy S, Rajalakshmi K, Zhu D, Zhao L, Wang S, Zhu W (2020) A novel lysosome targeted fluorophore for H_2S sensing: enhancing the quantitative detection with successive reaction sites. Sens Actuators B Chem 320:128433
10. Szabo C (2007) Hydrogen sulphide and its therapeutic potential. Nat Rev Drug Discov 6:917–935
11. Chen S, Li H, Hou P (2018) A novel imidazo[1,5-α]pyridine-based fluorescent probe with a large Stokes shift for imaging hydrogen sulfide. Sens Actuators B Chem 256:1086–1092
12. Skovgaard N, Gouliaev A, Aalling M, Simonsen U (2011) The role of endogenous H_2S in cardiovascular physiology. Curr Pharmaceut Biotechnol 12:1385–1393
13. Luo W, Xue H, Ma J, Wang L, Liu W (2019) Molecular engineering of a colorimetric two-photon fluorescent probe for visualizing H_2S level in lysosome and tumor. Anal Chim Acta 1077:273–280
14. Lee M, Schwab C, Yu S, McGeer E, McGeer P (2009) Astrocytes produce the antiinflammatory and neuroprotective agent hydrogen sulphide. Neurobiol Aging 30:1523–1534
15. Choi M, Cho M, Ryu H, Hong J, Chang S (2017) Fluorescence signaling of thiophenol by hydrolysis of dinitrobenzenesulfonamide of 2-(2-aminophenyl) benzothiazole. Dyes Pigm 143:123–128
16. Wang N, Wang H, Zhang J, Ji X, Su H, Liu J, Wang J, Zhao W (2022) Diketopyrrolopyrrole-based sensor for over-expressed peroxynitrite in drug-induced hepatotoxicity via ratiometric fluorescence imaging. Sens Actuators B Chem 352:130992
17. Fan G, Wang N, Zhang J, Ji X, Qin S, Tao Y, Zhao W (2022) BODIPY-based near-infrared fluorescent probe for diagnosis druginduced liver injury via imaging of HClO in cells and in vivo. Dyes Pigm 199:110073
18. Ren J, Zhang P, Liu H, Zhang C, Gao Y, Cui J, Chen J (2020) Single-dye-doped fluorescent nanoprobe enables self-referenced ratiometric imaging of hypochlorous acid in lysosomes. Sens Actuators B Chem 304:127299
19. Guo S, Leng T, Wang K, Wang C, Shen Y, Zhu W (2018) A colorimetric and turn-on NIR fluorescent probe based on xanthene system for sensitive detection of thiophenol and its application in bioimaging. Talanta 185:359–364
20. Chen S, Huang W, Tan H, Yin G, Chen S, Zhao K, Huang Y, Zhang Y, Li H, Wu C (2023) A large Stokes shift NIR fluorescent probe for visual monitoring of mitochondrial peroxynitrite during inflammation and ferroptosis and in an Alzheimer's disease model. Analyst. https://doi.org/10.1039/d3an00956d
21. Yin G, Gan Y, Jiang H, Yu T, Liu M, Zhang Y, Li H, Yin P, Yao S (2023) General Strategy for specific fluorescence imaging of Homocysteine in living cells and in vivo. Anal Chem 95:8932–8938
22. Li Y, Zhou Z, Chen S, Pang X, Wu C, Li H, Zhang Y (2023) Mitochondria-targeting fluorescent sensor with high photostability and permeability for visualizing viscosity in mitochondrial malfunction, inflammation, and AD models. Anal Chim Acta 1250:340967

23. Wang S, Xu S, Hu G, Bai X, James T, Wang L (2016) A fluorescent chemodosimeter for live-cell monitoring of aqueous sulphides. Anal Chem 88:1434–1439
24. Park C, Ha T, Choi S, Nguyen D, Noh S, Kwon O, Lee C, Yoon H (2017) A near-infrared turn-on fluorescent probe with a self-immolative linker for the in vivo quantitative detection and imaging of hydrogen sulfide. Biosens Bioelectron 89:919–926
25. Lv L, Luo W, Diao Q (2020) A novel ratiometric fluorescent probe for selective detection and imaging of H_2S. Spectrochim Acta A 246:118959
26. Guo M, Wang W, Ainiwaer D, Yang Y, Wang B, Yang J, Zhu H (2022) A fluorescent rhodol-derived probe for rapid and selective detection of hydrogen sulfide and its application. Talanta 237:122960
27. Ma Y, Wang X, Wang Z, Zhang G, Chen X, Zhang Y, Luo Y, Gao G, Zhou X (2023) A water-soluble NIR fluorescent probe capable of rapid response and selective detection of hydrogen sulfide in food samples and living cells. Talanta 256:124303
28. Lu T, Chen F (2012) Multiwfn: a multifunctional wavefunction analyzer. J Comput Chem 33:475–593
29. Manzetti S, Lu T (2013) The geometry and electronic structure of aristolochic acid: possible implications for a frozen resonance. J Phys Org Chem 26:473–483
30. Lu T, Manzetti S (2014) Wavefunction and reactivity study of benzo[a]pyrene diol epoxide and its enantiomeric forms. Struct Chem 25:1521–1533
31. Hirshfeld F (1977) Bonded-atom fragments for describing molecular charge densities. Theoret Chim Acta 44:129–138
32. Wang B, Wang X, Zeng A, Leng J, Zhao W (2021) Engineering a mitochondria-targeted ratiometric fluorescent probe with a large Stokes shift for H_2S-specific assaying in foodstuffs and living cells. Sens Actuators B Chem 343:130095